Experimental and Density-Functional-Theory (DFT) Studies on the DNA-Binding Trend and Spectral Properties of the Ruthenium Complexes $[Ru(4,7\text{-dmp})(bdip)]^{2+}$ and $[Ru(bpy)_2(bdip)]^{2+}$ (4,7-dmp = 4,7-Dimethyl-1,10-phenanthroline, bdip = 2-(1,3-Benzodioxol-4-yl)-1*H*-imidazo-[4,5-*f*][1,10]phenanthroline, bpy = 2,2′-bipyridine)

by **Li-Feng Tan***[a]), **Sheng Zhang**[a]), **Hui Chao**[b]), **Kang-Cheng Zheng**[b]), **Fang Wang**[a]), **Yue Xiao**[a]), and **Liang-Nian Ji**[b])

[a]) College of Chemistry, Xiangtan University, Xiangtan 411105, P. R. China (fax: 86-732-8292477; e-mail: lfwyxh@yahoo.com.cn)

[b]) Department of Chemistry, Sun Yat-Sen University, Guangzhou 510275, P. R. China

The new ligand bdip (= 2-(1,3-benzodioxol-4-yl)-1*H*-imidazo[4,5-*f*][1,10]phenanthroline) and its Ru^{II} complexes $[Ru(4,7\text{-dmp})_2(bdip)]^{2+}$ (**1**; 4,7-dmp = 4,7-dimethyl-1,10-phenanthroline) and $[Ru(bpy)_2(bdip)]^{2+}$ (**2**; bpy = 2,2′-bipyridine) were synthesized and characterized by elemental analysis, MS, ^{1}H-NMR, and cyclic voltammetry. The DNA-binding properties of **1** and **2** to calf-thymus DNA (CT-DNA) were investigated by different spectrophotometric methods and viscosity measurements as well as by equilibrium dialysis and circular-dichroism (CD) spectroscopy. The results suggest that both complexes bind to DNA through intercalation, and that the ancillary ligands of (polypyridine)ruthenium(II) complexes have significant effects on the spectral properties and DNA-binding behavior of the complexes. Theoretical studies for these complexes were also carried out by the density-functional-theory (DFT) method. The trend in the DNA-binding affinity and some electrochemical and spectral properties of the complexes were confirmed by the DFT calculations.

Introduction. – During the last decade, the interaction between transition-metal complexes and DNA has been extensively studied [1–8]. Binding studies of small molecules to DNA are very important in the development of new therapeutic reagents and DNA molecular probes [9–11]. (Polypyridine)ruthenium(II) complexes can bind to DNA by noncovalent interactions, such as by means of electrostatic binding, groove binding [12], and intercalative and partial intercalative binding [13][14]. Since many useful applications require that the complexes bind to DNA in an intercalative mode, much work has been done on modifying the intercalative ligands [15]. However, the influence of ancillary ligands of the complexes has received little attention. Since the octahedral (polypyridine)ruthenium(II) complexes bind to DNA in three dimensions, the ancillary ligands can also play an important role in governing the DNA binding. Therefore, it is worthwhile to explore the effects of ancillary ligands on the interaction and the binding mode of metal complexes to DNA. To understand clearly the effects of ancillary ligands, the selection of the intercalative ligand is also very important. An appropriate intercalative ligand can help to distinguish the small differences of interaction with DNA of complexes containing different ancillary ligands.

[Ru^{II}(polypyridine)] complexes with intercalative and ancillary ligands have been synthesized and experimentally studied, but theoretical reports on them are relatively scarce. To discuss the interaction mechanism between the complex and DNA and to further guide the molecular design of such a type of complexes, theoretical studies are very helpful. At present, various attempts to correlate experimental results in this field to theoretical predictions have been carried out. In particular, quantum-chemical studies applying the density-functional theory (DFT) have been reported [16], because the DFT can better consider electron correlation energies, reduces the computation expenses, and is appropriate to compute, in the case of such complexes, singlet ground states. It is well documented that the lowest-energy transition of some [Ru^{II}(polypyridine)] complexes can be assigned to a metal-to-ligand charge transfer (MLCT), and the HOMO–LUMO energy difference for different corresponding complexes, calculated by the DFT/B3LYP method, is closely correlated to $\Delta E_{1/2}$ ($E_{1/2ox} - E_{1/2red}$) [17]. DFT Calculations for the stacked DNA base-pair model with backbones have also been reported, and it is well established that the energies of the HOMO and the occupied MO near HOMO are rather high, these MOs being predominantly populated on the base pairs of DNA [18].

Herein, we report the synthesis and characterization of 2-(1,3-benzodioxol-4-yl)-1*H*-imidazo[4,5-*f*][1,10]phenanthroline (bdip), a new polypyridine ligand, and its Ru^{II} complexes $[Ru(4,7\text{-dmp})_2(bdip)]^{2+}$ (**1**; 4,7-dmp = 4,7-dimethyl-1,10-phenanthroline) and $[Ru(bpy)_2(bdip)]^{2+}$ (**2**; bpy = 2,2′-bipyridine). The DNA-binding properties of the two complexes were explored by spectroscopic and viscosity measurements as well as by equilibrium dialysis and circular-dichroism (CD) spectroscopy. Theoretical calculations by the DFT for the two complexes were also carried out and used to explain the experimental observations. The results contribute to the understanding of the selectivity and efficiency of DNA recognition by different (polypyridine)ruthenium(II) complexes; development of new DNA photoprobes and photoreagents.

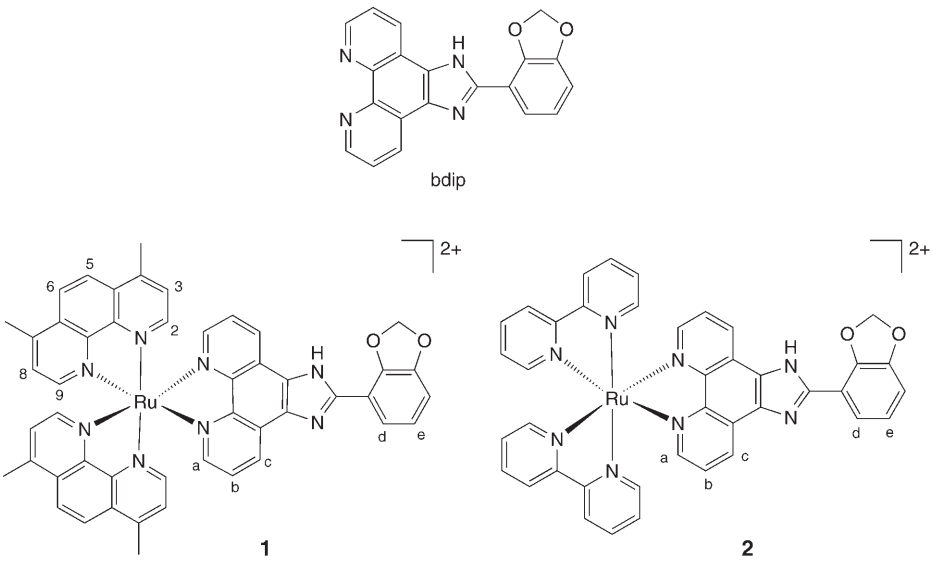

Results and Discussion. – 1. *Ru^{II} Complexes* **1** *and* **2**. First the new ligand bdip was prepared by condensation of 1,10-phenanthroline-5,6-dione (**3**) with 1,3-benzodioxole-4-carboxaldehyde (**4**) according to the method for the preparation of imidazole rings developed by *Steck* and *Day* [19]. The complexes $[Ru(4,7\text{-dmp})_2(bdip)]^{2+}$ (**1**) and $[Ru(bpy)(bdip)_2]^{2+}$ (**2**) were then obtained in 67 and 62% yield, respectively, by direct reaction of bdip with *cis*-$[Ru(4,7\text{-dmp})_2Cl_2]\cdot 2\,H_2O$ and *cis*-$[Ru(bpy)_2Cl_2]\cdot 2\,H_2O$ in ethane-1,2-diol (*Scheme*). The complexes **1** and **2** were isolated as perchlorates, purified by column chromatography, and identified by their MS and ^{1}H-NMR data. In the ESI-MS of the perchlorates of **1** and **2**, the ions $[M-ClO_4^-]^+$, $[M-2\,ClO_4-H]^+$, and $[M-2\,ClO_4^-]^{2+}$ were observed, and the determined molecular masses were consistent with expected values. Both **1** and **2** gave well-defined ^{1}H-NMR spectra (*Fig. 1*), permitting unambiguous identification and assessment of purity. The chemical shifts were assigned by ^{1}H,^{1}H-COSY experiments and by comparison with the values of similar compounds [20–23]. Due to the shielding influences of the adjacent bdip and 4,7-dmp (or bpy), the 4,7-dmp (or bpy) H-atoms of **1** and **2** exhibited two distinct sets of signals. In addition, the NH of bdip was not observed due to rapid H^+ exchange between the two N-atoms of the imidazole ring. A similar case has been reported previously [21][22].

Scheme. *Synthesis of the Ligand bdip and of Its Ru^{II} Complexes* **1** *and* **2**

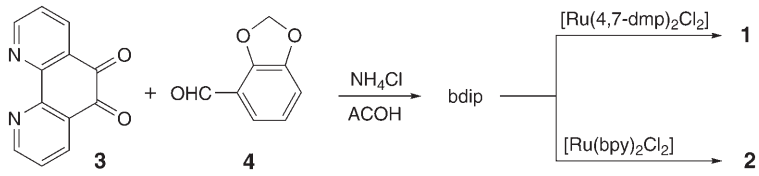

The UV/VIS absorption spectra of **1** and **2** showed three well-resolved bands in the range 200–600 nm, characterized by intense $\pi\rightarrow\pi^*$ ligand transitions in the UV, as well as by a metal-to-ligand charge transfer (MLCT) transition in the VIS. The broad MLCT absorption bands appeared at 434 and 456 nm for **1** and **2**, respectively, and are attributed to $Ru(d\pi)\rightarrow$ bdip (π^*) transitions. These bands are bathochromically shifted relative to those of $[Ru(bpy)_3]^{2+}$ (452 nm) [24], in accord with the extension of the corresponding π framework. The peak below 400 nm was assigned to the internal $\pi\rightarrow\pi^*$ transition of the ligands, by comparison with the spectra of $[Ru(bpy)_3]^{2+}$. The results indicate that, for complex **1**, the incorporation of electron-donating Me groups at C(4) and C(7) of the phen ligand shifts the MLCT band to shorter wavelength. A similar case has been found with other analogues previously [24].

The electrochemical behavior of the complexes was determined in MeCN. Each complex exhibited one oxidation and three reduction waves in the sweep range -2.0 to $+2.0$ V, the half-wave potentials $E_{1/2}$ being 1.45, -0.61, -1.43, and -1.71 V *vs.* SSCE for complex **1**, and 1.52, -1.17, -1.34, and -1.75 V for complex **2**. The electrochemical behavior of [Ru^{II}(polypyridine)] complexes has been rationalized in terms of a metal-based oxidation and a series of reductions which are ligand-based occurring in a stepwise manner for each π^* system [21]. As expected, the oxidation potentials of complex **1** and **2** were more positive than that of $[Ru(bpy)_3]^{2+}$, in accord with the

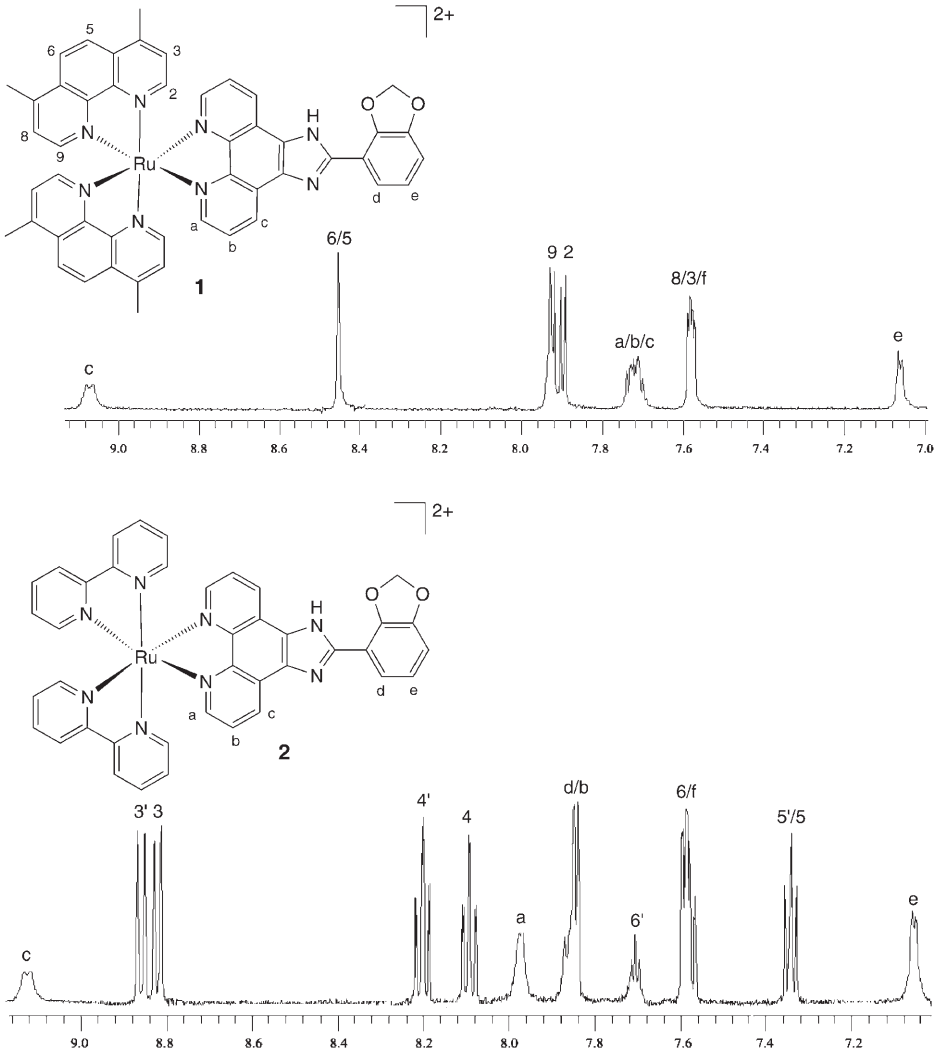

Fig. 1. *^{1}H-NMR Signals* ((D_6)DMSO; 400 MHz) *of the aromatic protons of complex* **1** (top) *and complex* **2** (bottom)

extension of the corresponding π framework. With reference to previous studies on similar systems [22][23], the first reduction, which is usually controlled by the ligand having the lowest unoccupied molecular orbital (LUMO) [25], is assigned to a reduction centered on bdip, and the last reductions are characteristic of the co-ligand (4,7-dmp or bpy) [26].

The trend in the electrochemical half-wave potentials of **1** and **2** was supported by the energy diagram of the frontier molecular orbitals obtained from the DFT calculations. The stereographs of the related frontier molecular orbitals of **1** and **2** are given in the *Table* and *Figs. 2* and *3*. We can see that the MO characterized by the metal

Table. *Some Frontier-Molecular-Orbital Energies* ε [atomic unit] *of Complexes* **1** *and* **2**

Comp.	Occ[a])	Occ	HOMO	LUMO	Vir[b])	Vir	$\Delta\varepsilon_{L-H}$[c])	$\Delta\varepsilon_{L-NH}$[c])	$\Delta\varepsilon_{L-(H-2)}$[c])
1	−0.3955	−0.3750	−0.3586	−0.2727	−0.2694	−0.2626	0.0859	0.0892	0.1228
2	−0.3796	−0.3680	−0.3536	−0.2538	−0.2506	−0.2498	0.0998	0.1030	0.1258

[a]) Occ = occupied molecular orbital; HOMO (or H) = the highest Occ. [b]) Vir = virtual molecular ortibal; LUMO (or L) = the lowest Vir. [c]) $\Delta\varepsilon_{L-H}$ = energy difference between LUMO and HOMO; $\Delta\varepsilon_{L-NH}$ = energy difference between LUMO and NHOMO (= next HOMO or NH); $\Delta\varepsilon_{L-(H-2)}$ = energy difference between LUMO and NHOMO-2 (or H-2).

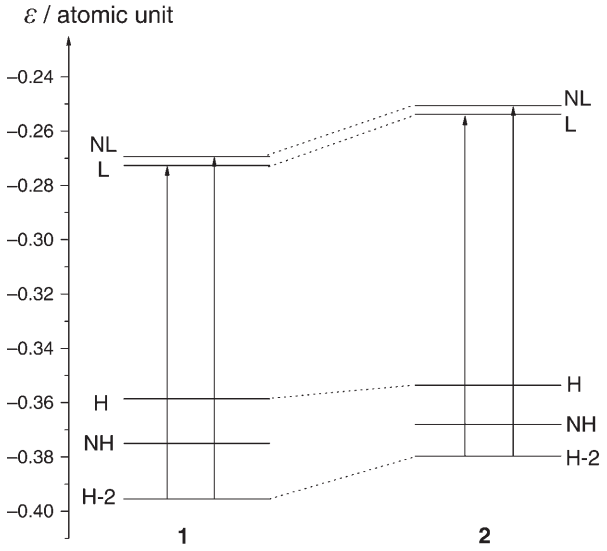

Fig. 2. *Schematic diagram of energies and related* ^{1}*MLCT transitions of complexes* **1** *and* **2**

d-orbital in the occupied frontier MO is NHOMO-2 (= H-2) instead of HOMO (= H), so that the oxidation of the central metal should happen on the NHOMO-2 (see *Fig. 3*). Since the NHOMO-2 energy of complex **2** is lower than that of complex **1** (see *Table* and *Fig. 2*), the oxidation potential of **2** is more positive than that of **1**. On the other hand, since the LUMO is playing an electron-accepting role, and the LUMO energy of complex **2** is also lower than that of complex **1**, the reduction potential of **2** is more negative than that of **1**.

2. *DNA Binding.* 2.1. *UV/VIS Titration.* The application of electronic absorption spectroscopy in DNA-binding studies is one of the most useful techniques [27]. Complex binding with DNA through intercalation usually results in hypochromism and bathochromism, due to the intercalative mode involving a strong stacking interaction between an aromatic chromophore and the base pairs of DNA. The extent of the hypochromism commonly parallels the intercalative binding strength.

In *Fig. 4*, the absorption spectra of the Ru^{II} complexes **1** and **2** (at a constant concentration) are shown in the absence and presence of CT-DNA. As can be seen for

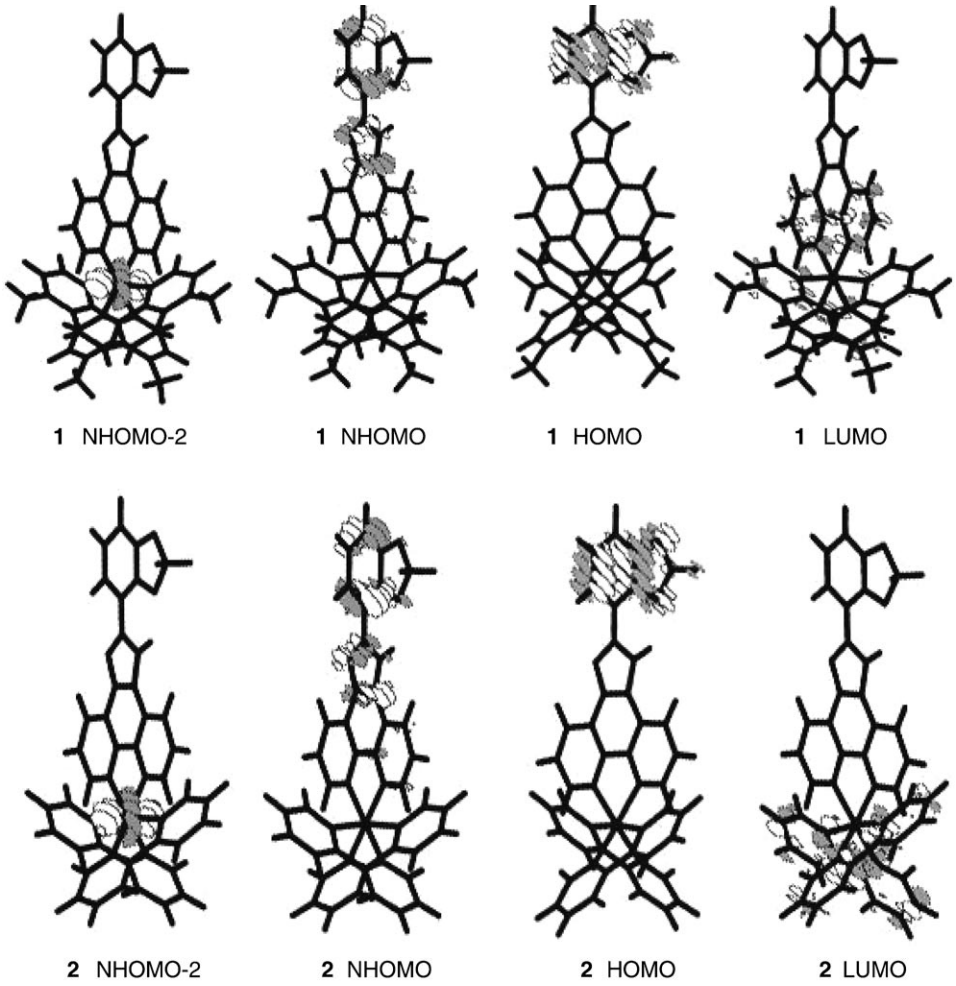

Fig. 3. *Some frontier-molecular-orbital stereographs of complexes* **1** *and* **2** (*cf. Fig. 2* and *Table*)

complex **1**, upon increasing the CT-DNA concentration, the hypochromism at 440 nm (MLCT band) reaches 20.8%, with a red shift of 5 nm at a [DNA]/[Ru] ratio of 7.6. For complex **2**, under the same experimental conditions, the MLCT band at 470 nm shows hypochromism of *ca.* 33%, and a red shift of 11 nm at a [DNA]/[Ru] ratio of 11.88. Comparing the hypochromism of **1** or **2** with that of the parent complex $[Ru(phen)_3]^{2+}$ (12% hypochromism for the MLCT band at 445 nm, 2 nm of red shift) [15], which interacts with DNA through a semi-intercalation or quasi-intercalation [28] and considering that the absorption spectrum of $[Ru(bpy)_3]^{2+}$, a typical electrostatically binding complex, was unchanged upon the addition of DNA [12], these spectral characteristics obviously suggest that the two complexes **1** and **2** interact with DNA by a stacking interaction between the aromatic chromophore and the base pairs of DNA. The spectra also imply that complex **2** binds more strongly to DNA than complex **1**.

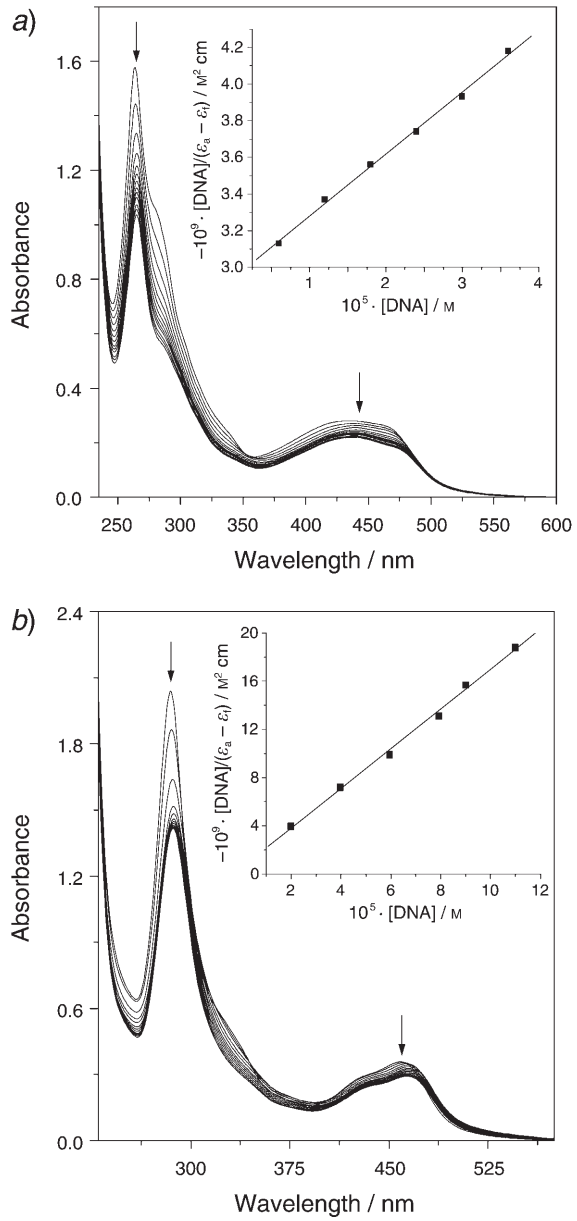

Fig. 4. *Absorption spectra of* a) *complex* **1** b) *and complex* **2** *in aqueous* Tris · *HCl buffer upon addition of CT-DNA*. [Ru] = $2 \cdot 10^{-5}$ M, [DNA] = $(0-23.76) \cdot 10^{-5}$ M. The arrows show the absorbance changes upon increasing DNA concentration. Inset: plots of $-10^9 \cdot [DNA]/(\varepsilon_a - \varepsilon_f)$ (in $M^2 \cdot cm$) *vs.* [DNA] (in M) for the titration of DNA with the complex for the determination of the binding constant K_b.

To quantitatively compare the DNA-binding strengths of **1** and **2**, their intrinsic binding constants K_b were determined by UV/VIS titration. This was done by monitoring the changes in absorbance at 440 nm for **1**, and at 470 nm for **2**, with increasing concentration of DNA, and by using *Eqn. 1* [29], wherein [DNA] is the concentration of DNA in base pairs, ε_a, ε_f, and ε_b are the apparent-, free-, and bound-metal-complex extinction coefficients, respectively. When plotting $[DNA]/(\varepsilon_a - \varepsilon_f)$ *vs.* [DNA], K_b is given by the ratio of the slope to the intercept. The intrinsic binding constants K_b of complexes **1** and **2** were, thus, determined as $(1.15 \pm 0.12) \cdot 10^4$ M^{-1} and $(3.25 \pm 0.23) \cdot 10^4$ M^{-1}, respectively. The results indicate that, as the ancillary ligand varies from bpy to 4,7-dmp, the DNA binding affinity of the Ru^{II} complexes declines. For comparison, the intrinsic binding constants K_b of typical 'intercalative-type' Ru^{II} complexes is in the range of $1.1 \cdot 10^4 - 4.8 \cdot 10^4$ M^{-1} [30], whereas that of the parent complex $[Ru(phen)_3]^{2+}$ is $5.5 \cdot 10^3$ M^{-1} [30a]. Hence, complex **1** and **2** clearly bind to DNA by intercalation, **2** having a higher affinity than **1**, in accord with the above UV/VIS studies. Since the intercalative ligands of both complexes are the same, the differences of the DNA-binding affinity is attributed to the ancillary-ligand effects.

$$[DNA]/(\varepsilon_a - \varepsilon_f) = [DNA]/(\varepsilon_b - \varepsilon_f) + 1/[K_b(\varepsilon_b - \varepsilon_f)] \quad (1)$$

2.2. *Fluorescence Quenching*. Luminescene spectroscopy is one of the most common and at the same time most sensitive ways to analyze drug–DNA interactions. Support for the above intercalative binding mode also comes from the emission measurement of both complexes. In the absence of DNA, complexes **1** and **2** are luminescent in *Tris* buffer at room temperature, with the fluorescence maximum at 609 and 596 nm, respectively. As shown in the steady-state luminescene spectra of 2 μM solutions of **1** and **2** in the presence of CT-DNA (*Fig. 5*), the luminescene intensities increased by a factor of *ca*. 3.42 and 4.91, and saturated at a [DNA]/[Ru] ratio of 47.25 and 54, respectively. This indicates that both complexes **1** and **2** strongly interact with DNA, which efficiently 'protects' them, since the hydrophobic environment inside the DNA helix reduces the accessibility of solvent H_2O molecules to the complex, and because complex mobility is restricted at the binding site, factors that result in a decrease of the vibrational modes of relaxation and, thus, in higher emission intensity.

Steady-state luminescene-quenching experiments with $[Fe(CN)_6]^{4-}$ as quencher may provide further information about complexes binding to DNA but cannot determine the binding mode. We decided to perform some experiments at room temperature, using a similar method as that described by *Chaires* and co-workers [31]. Thus, at constant ionic strength, KCl was added along with $K_4[Fe(CN)_6]$. As illustrated in *Fig. 6*, the fluorescence-quenching curves at constant ionic strength were nonlinear. For complex **1** and **2**, the final fluorescence intensities were originally 77.70 and 82.40%, respectively. These results, thus, further confirm that complex **2** binds more strongly to DNA than **1**.

2.3. *Viscosity Measurements*. Hydrodynamic measurements sensitive to length changes, as reflected in viscosity and sedimentation, are regarded as the least ambiguous and the most critical tests of a binding model in solution in the absence of crystallographic structural data [32]. A classical intercalation model demands that the

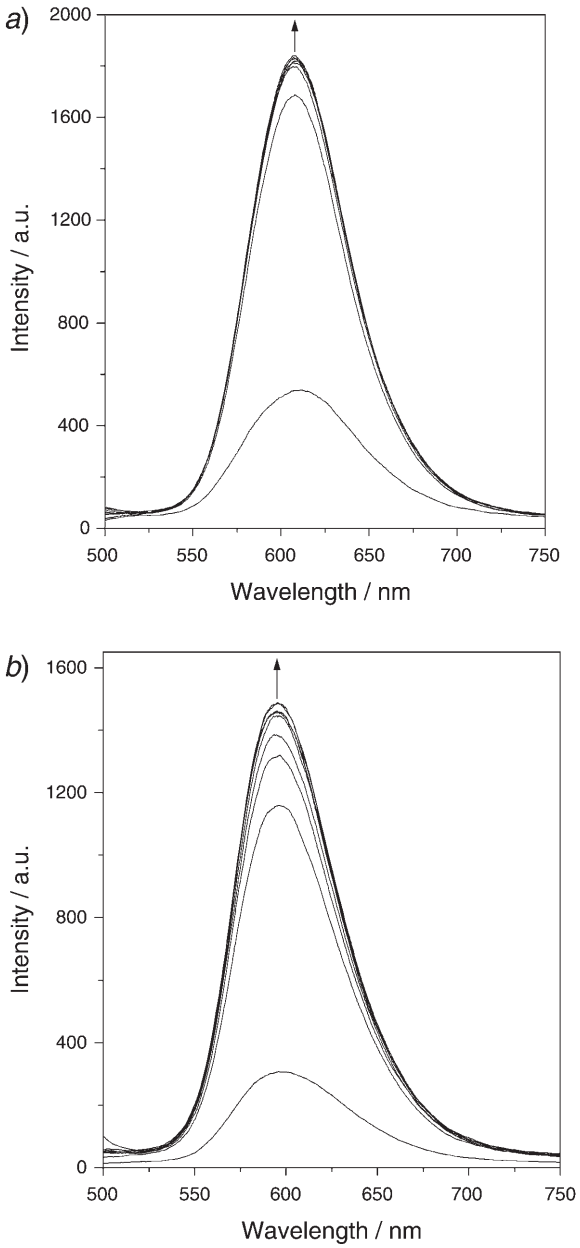

Fig. 5. *Fluorescence spectra of* a) *complex* **1** *and* b) *complex* ***2*** *in aqueous* Tris · *HCl buffer at 298 K in the presence of CT-DNA*. The arrows show the intensity changes upon increasing DNA concentrations. $[Ru] = 2 \cdot 10^{-6}$ M, [DNA]/[Ru] = 47.25 and 54 for **1** and **2**, resp., at saturation.

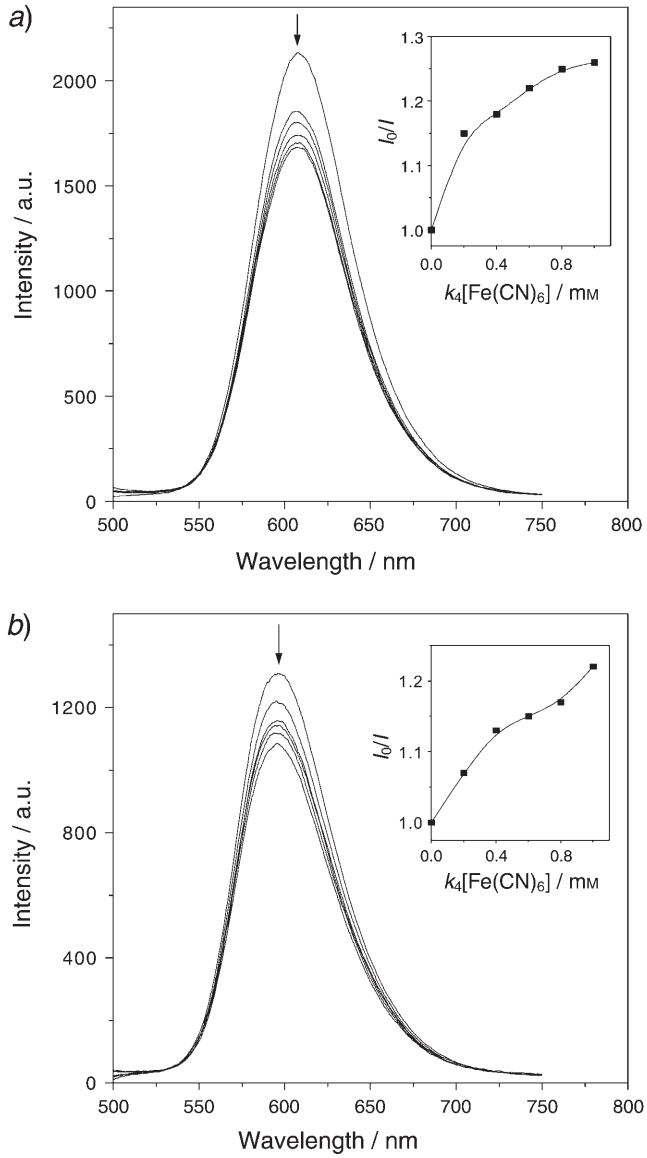

Fig. 6. *Fluorescence quenching of* a) *complex* **1** *and* b) *complex* **2** *in the presence of DNA by* $[Fe(CN)_6]^{4-}$. $[Ru] = 2 \cdot 10^{-6}$ M, $[DNA]/[Ru] = 40$, $[K^+] = 4 \cdot 10^{-3}$ M. $[Fe(CN)_6]^{4-} = 0 \rightarrow 1.0$ mM (arrows). Inset: plots of I_0/I *vs.* $[Fe(CN)_6]^{4-}$ (in mM), where I_0 and I are the fluorescence intensities in the absence and presence of the quencher, resp.

DNA helix lengthens as base pairs are separated to accommodate the binding ligand, which, in turn, leads to an increase in the viscosity of DNA [32].

In *Fig. 7*, the changes in viscosity on rod-like DNA is shown in the presence of complexes **1** and **2**, $[Ru(bpy)_3]^{2+}$ and ethidium bromide (= 3,8-diamino-5-ethyl-6-

phenylphenanthridinium bromide; EB). Whereas EB, a well-known DNA intercalator, gave rise to a strong change in DNA viscosity upon complexation, $[Ru(bpy)_3]^{2+}$, which binds by electrostatic interactions only, exerted essentially no such effect. As can be seen from *Fig. 7*, upon increasing the amount of **1** or **2**, the relative viscosity of DNA increased steadily, similarly to in the case of EB. The increase of the relative viscosity, expected to correlate with the DNA-intercalating potential of a compound, followed the order EB > **2** > **1**. These results suggest that complexes **1** and **2** both bind to DNA through intercalation, the difference in binding strength probably being caused by the different ancillary ligands. The four additional Me groups in **1** relative to **2** may exert much more steric hindrance. Therefore, complex **2** is probably more deeply intercalated and more tightly bound to adjacent DNA base pairs than complex **1**.

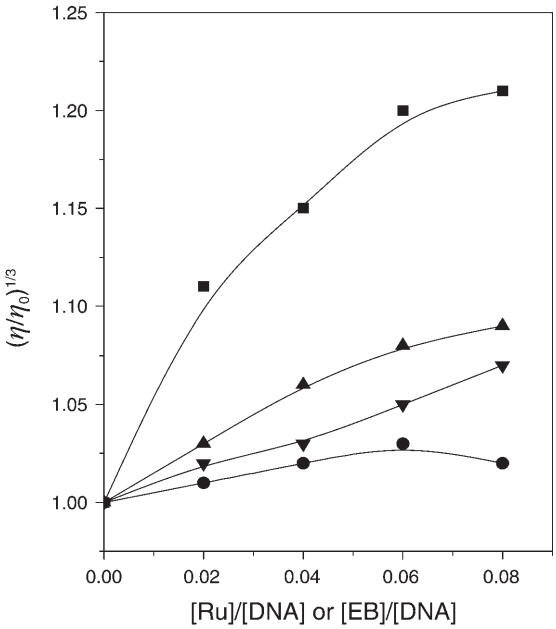

Fig. 7. *Effect of increasing amounts of ethidium bromide* (■), *$[Ru(bpy)_3]^{2+}$* (●), **1** (▼), *and* **2** (▲) *on the relative viscosity of CT-DNA*. Total DNA concentration 0.5 mM, *T* 30 ± 0.1°.

2.4. *Enantioselective DNA Binding.* Equilibrium dialysis experiments offer the opportunity to examine the enantioselectivity of complexes binding to DNA. According to the proposed binding model by *Barton* and co-workers [33], the Δ enantiomer of the complex, a right-handed propeller-like structure, displays a greater affinity than the Λ enantiomer with the right-handed CT-DNA helix due to a better steric matching. Thus, racemic solutions of the two complexes were dialyzed against CT-DNA for 42 h and then subjected to circular-dichroism (CD) analysis. In *Fig. 8*, the CD spectra in the UV region of the dialysates of **1** and **2** are shown. The dialysate of complex **1** (solid line) shows two strong CD signals with a positive peak at 272 and a negative peak at 255 nm, while complex **2** (dotted line) shows strong CD signals with a positive peak at 276 nm and a negative peak at 294 nm. Furthermore, the CD signals of

complex **1** are in opposition to those of complex **2**. The stronger CD signals of complex **1** suggest a large DNA-binding discrimination between its two antipodes. It is likely that for the more weakly DNA-binding complex **1**, the steric hindrance of the Me groups of the 4,7-dmp ligand has a very important effect on one of the enantiomers binding to DNA, thus leading to a special preference for the other enantiomer to bind to DNA. These results establish a significant influence of the ancillary ligands on the enantioselectivity of (polypyridine)ruthenium(II) complexes during binding to DNA. Although neither of the complexes was resolved into the pure enantiomers, and we cannot determine which enantiomer binds preferentially to CT-DNA, it is evident that both **1** and **2** interact enantioselectivly with CT-DNA.

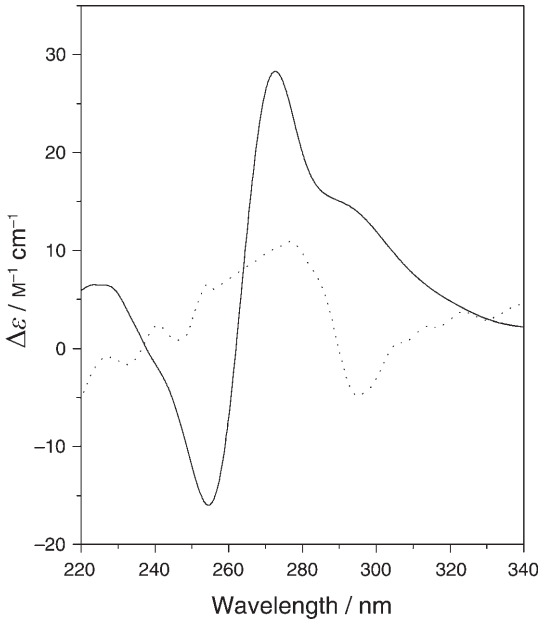

Fig. 8. *CD Spectra of* **1** (—) *and* **2** (···) *after 42 h of dialysis against CT-DNA in stirred aqueous solution*

2.5. *Theoretical Support of Trends in DNA-Binding and Spectral Properties of Complexes.* As it is well known, there are $\pi-\pi$ interactions in the DNA-binding of complexes by the intercalation mode. Due to the large size of the supramolecular system formed from DNA and the complex **1** or **2**, their interaction can only be estimated from the individual electronic structural characteristics by means of the DFT and the frontier-molecular-orbital theory [34]. Some computed frontier molecular energies, the schematic diagram of the ^{1}MLCT transition, and the stereographs of the related frontier molecular orbitals of both complexes are given in the *Table* and *Figs. 2* and *3*, respectively. According to the frontier-molecular-orbital theory, a reaction controlled by orbital interactions between two molecules is favored by a higher HOMO energy of one molecule and a lower LUMO energy of the other molecule. A simple and reasonable calculation model and results computed by the DFT method for stacked DNA base pairs with backbone have been reported by *Kurita et al.* [18]. The reported

HOMO and NHOMO energies of the DNA-section model are much higher (−1.27 and −2.08 eV) [35] than our calculated LUMO and NLUMO energies (*ca.* −0.26 eV) of the complexes **1** and **2** (*Table*). Presumably, the order of magnitude of the (relative) energy gap is similar in the present DNA/complex system; thus the attraction of a metal-complex cation with a high positive charge for electrons in the frontier MOs is much stronger than that of various DNA. Furthermore, the 'electronic cloud' of the HOMO and NHOMO of the DNA model is predominantly located on the base pairs, whereas the 'electronic cloud' of the LUMO and NLUMO (if they have accepted electrons) of the metal complex is mainly distributed over the intercalative ligand bdip. Such orbital distributions are advantageous for an orbital overlap between the HOMO of DNA and the LUMO of the metal complex in an intercalative mode, suggesting that the $\pi-\pi$ interaction in the intercalation mode is due to the electron flow from the HOMO of DNA populated on the base pairs to the LUMO of the metal complex of lower energy. Therefore, a lower LUMO energy of the metal complex should favor the electron flow from the base pairs of DNA in the intercalation mode, and the LUMO energy of the metal complex should be an important factor (but not the only one) correlating to its DNA-binding constant K_b. The experimental results established indeed that $K_b(\mathbf{2}) > K_b(\mathbf{1})$. The hydrophobicity of the 4,7-dmp ligand of **1** is greater than that of the bpy ligand of **2**, and the LUMO energy of **2** (−0.2727 atomic unit) is lower than that of **1** (−0.2506 atomic unit) (see *Table 1* and *Fig. 2*). As a result, $K_b(\mathbf{2}) > K_b(\mathbf{1})$ when considering both the LUMO energy factor and the hydrophobicity effect of the ancillary ligand.

Fig. 3 clearly shows that the metal-to-ligand charge-transfer (^{1}MLCT) band (λ_{max}) for complexes **1** and **2** should correspond to the electron transition from their NHOMO-2 to LUMO, according to the molecular-orbital components of the complexes.

In addition, the absorption spectra of **1** and **2** also demonstrate that the corresponding energy difference in the presence and absence of DNA is small (*Fig. 4*) and no special pattern changes in the spectra in the presence of DNA can be detected, except for the increase in hypochromism. Therefore, the corresponding orbital of the complexes **1** and **2** is not much affected on binding to DNA. This further suggests that the interaction between the complex **1** or **2** and DNA should be a weak one, so that the property and assignment of the ^{1}MLCT band of **1** and **2** should be unchanged on binding to DNA, which is in accord with experiments.

3. Conclusions. – In summary, the two novel complexes $[Ru(4,7\text{-dmp})_2(bdip)]^{2+}$ (**1**) and $[Ru(bpy)_2(bdip)]^{2+}$ (**2**) were synthesized and characterized. Their DNA-binding properties were investigated. Spectroscopic studies, viscosity measurements, as well as equilibrium dialysis and CD spectroscopy established that **1** or **2** bind to CT-DNA through intercalation and in an enantioselective way. Complex **1** is a much better enantioselective binder to CT-DNA than complex **2**. The experimental results suggested that the ancillary ligands of (polypyridine)ruthenium(II) complexes affect significantly their spectral properties and DNA-binding behavior. The DFT calculations confirmed the experimentally determined trend in the binding strength or binding constants (K_b) of the complexes **1** and **2** to DNA and roughly predicted some of their spectral properties.

The authors thank the *Provincial Natural Science Found of Hunan* (06JJ5023), the *Scientific Research Found of Hunan Provincial Education Department* (06C828), and the *Doctoral Foundation of Xiangtan University* (05QDZ11) for their support of this research.

Experimental Part

General. All reagents and solvents were commercially available and used without further purification, unless otherwise noted. Doubly distilled H_2O was used to prepare buffers. CT-DNA was obtained from the *Sino-American Biotechnology Company.* The compounds 1,10-phenanthroline-5,6-dione [36], *cis*-$[Ru(4,7\text{-dmp})_2Cl_2]\cdot 2\,H_2O$ [37] and *cis*-$[Ru(bpy)_2Cl_2]\cdot 2\,H_2O$ [38] were prepared according to the literature. Other materials were commercially available and reagent grade. UV/VIS Spectra: *Perkin-Elmer Lambda-25* apparatus; λ_{max} in nm, ε in $dm^3\ mol^{-1}\ cm^{-1}$. Fluorescenc spectra: *Perkin-Elmer LS-55* spectrophotometer; at r.t. CD Spectra: *Jasco J715* spectropolarimeter. ^{1}H-NMR Spectra: *Bruker Avance-400* apparatus; at 400 MHz in D_6(DMSO) at r.t.; δ in ppm rel. to Me_4Si, *J* in Hz. FAB-MS: *VG-ZAB-HS* mass spectrometer; 3-nitrobenzyl alcohol (NBA) matrix. ESI-MS: *LQC* system (*Finnigan MAT*), with MeCN as mobile phase; spray voltage 4.50 KV, tube-lens offset 30.00 V, capillary voltage 23.00 V, and capillary temp. 200°; in *m*/*z*. Elemental analyses: *Perkin-Elmer 240Q* elemental analyzer.

*2-(1,3-Benzodioxol-4-yl)-1*H-*imidazo[4,5-*f*][1,10]phenanthroline* (bdip). A mixture of 1,3-benzodioxole-4-carboxaldehyde (=(2,3-methylenedioxy)benzaldehyde; 0.23 g, 1.5 mmol), 1,10-phenanthroline-5,6-dione (0.11 g, 0.5 mmol), NH_4OAc (2.31 g, 30 mmol) and AcOH (15 ml) was refluxed with stirring for 2 h. The cooled soln. was filtered, diluted with H_2O, and neutralized with conc. aq. NH_3 soln. The yellow precipitate was collected and purified by column chromatography (CC; *Alox*, EtOH/toluene 4:1): bdip (0.21 g, 41%). FAB-MS: 341.6 ($[M+1]^+$). Anal. calc. for $C_{20}H_{13}N_4O_2$: C 68.75, H 3.72, N 16.04; found C 68.34, H 3.91, N 15.70.

*[2-(1,3-Benzodioxol-4-yl)-1*H-*imidazo[4,5-*f*][1,10]phenanthroline-*$\kappa N^7,\kappa N^8$*]bis(4,7-dimethyl-1,10-phenantholine-*$\kappa N^1,\kappa N^{10}$*)ruthenium(2+) Diperchlorate Dihydrate* ($[Ru(4,7\text{-dmp})_2(bdip)](ClO_4)_2\cdot 2\,H_2O$; $\mathbf{1}\cdot 2ClO_4^-\cdot 2\,H_2O$). A mixture of *cis*-$[Ru(4,7\text{-dmp})_2Cl_2]\cdot 2\,H_2O$ (147 mg, 0.25 mmol), bdip (85 mg, 0.25 mmol), and ethane-1,2-diol (15 ml) was thoroughly deoxygenated. The purple mixture was heated for 8 h at 120° under Ar. When the soln. finally turned red, it was cooled to r.t., and an equal volume of sat. aq. $NaClO_4$ soln. was added under vigorous stirring. The red solid was collected and washed with small amounts of H_2O, EtOH, and Et_2O, dried under vacuum, and purified by CC (neutral *Alox*, MeCN/toluene 2:1): 190 mg (67%) of $\mathbf{1}\cdot 2ClO_4^-\cdot 2\,H_2O$. UV/VIS (MeCN): 434 (15780), 264 (50730), 230 (39830). ^{1}H-NMR (400 MHz, (D_6)DMSO; arbitrary atom numbering, see **1**): 9.07 (*d*, *J* = 7.5, 2 H, H_c); 8.45 (*s*, 4 H, H–C(5), H–C(6)); 8.28 (*s*, 2 H, H_a); 7.92 (*d*, *J* = 5, 2 H, H–C(9)); 7.90 (*d*, *J* = 5, 2 H, H–C(2)); 7.70–7.74 (*m*, 6 H, H_b, H–C(8), H–C(3)); 7.57–7.59 (*m*, 2 H, H_f, H_d); 7.06 (*d*, *J* = 5.5, 1 H); 6.25 (*s*, 1 H, H_g). ESI-MS (MeCN): 957.1 ($[M-ClO_4]^+$), 857.5 ($[M-2\ ClO_4-H]^+$), 429.2 ($[M-2\ ClO_4]^{2+}$). Anal. calc. for $C_{48}H_{40}Cl_2N_8O_{11}Ru$: C 54.29, H 3.26, N 10.34; found: C 54.11, H 3.36, N 10.17.

*[2-(1,3-Benzodioxol-2-yl)-1*H-*imidazo[4,5-*f*][1,10]phenanthroline-*$\kappa N^7,\kappa N^8$*]bis(2,2′-bipyridine-*$\kappa N^1,\kappa N^{1'}$*)ruthenium(2+) Diperchlorate Dihydrate* ($[Ru(bpy)_2(bdip)](ClO_4)_2\cdot 2\,H_2O$; $\mathbf{2}\cdot 2ClO_4^-\cdot 2\,H_2O$). As described for **1**, with *cis*-$[Ru(bpy)_2Cl_2]\cdot 2\,H_2O$ (130 mg, 0.25 mmol): 150 mg (62%) of $\mathbf{2}\cdot 2ClO_4^-\cdot 2\,H_2O$). UV/VIS (MeCN): 456 (16430), 286 (68537), 240 (33410). ^{1}H-NMR (400 MHz, (D_6)DMSO; arbitrary atom numbering, see **2**): 9.12 (*d*, *J* = 7, 2 H, H_c); 8.86 (*d*, *J* = 6.4, 2 H, H–C(3′)); 8.82 (*d*, *J* = 6.8, 2 H, H–C(3)); 8.20 (*t*, 2 H, H–C(4′)); 8.09 (*t*, 2 H, H–C(4)); 7.97 (*d*, *J* = 6.4, 2 H, H_a); 7.85 (*t*, 3 H, H_d, H_b); 7.71 (*t*, 2 H, H–C(6′)); 7.56–7.59 (*m*, 3 H, H–C(6), H_f); 7.320–7.36 (*m*, 4 H, H–C(5′), H–C(5)); 7.06 (*d*, *J* = 3.2, 1 H, H_e); 6.25 (*s*, 1 H, H_g). ESI-MS (MeCN): 853.0 ($[M-ClO_4]^+$), 753.2 ($[M-2\ ClO_4-H]^+$), 377.3 ($[M-2\ ClO_4]^{2+}$). Anal. calc. for $C_{40}H_{32}Cl_2N_8O_{12}Ru$: C 48.60, H 3.24, N 11.33; found: C 48.36, H 3.39, N 11.15.

Cyclic Voltammetry. An *EG&G-PAR-273* polarographic analyzer and *270* universal programmer were used. The supporting electrolyte was 0.1M $(Bu_4N)ClO_4$ in MeCN freshly distilled from P_2O_5 and deaerated by purging with N_2. A standard three-electrode system comprising a Pt-microcylinder working electrode, a Pt-wire auxiliary electrode, and a saturated calomel reference electrode (SCE) was used.

UV/VIS Titrations. All experiments were carried out in buffer *A* (5 mM *Tris* · HCl, 50 mM NaCl, pH 7.2) at r.t. A soln. of CT-DNA in buffer *A* gave a ratio of UV absorbances at 260 and 280 nm of *ca.* 1.8 : 1 to 1.9 : 1, indicating that the DNA was sufficiently free of protein [39]. The concentration of CT-DNA was determined spectrophotometrically (ε_{260} 6600 cm^{-1}) [40]. Stock solns. were stored at 4° and used within 4 d. Titration experiments were performed by using a fixed Ru^{II}-complex concentration (10 μM), to which CT-DNA stock solns. were added up to a ratio of [DNA]/[Ru] 2 : 1. The complex/DNA solns. were allowed to equilibrate for 5 min before spectra were recorded.

Viscosity Measurements. An *Ubbelodhe* viscometer was maintained at a const. temp. of 30.0 ± 0.1° in a thermostatic bath. DNA Samples of an average length of *ca.* 200 base pairs were prepared by sonication [41]. The flow time was measured with a digital stopwatch, and each sample was tested three times to get an average calculated time. Data are presented as $(\eta/\eta_0)^{1/3}$ *vs.* the binding ratio [42], where η is the viscosity of DNA in the presence of complex and η_0 the viscosity of free DNA.

Theoretical Calculations. Each complex **1** or **2** contains a Ru^{II} ion, one main ligand or intercalative ligand (bdip), and two ancillary ligands (4,7-dmp or bpy). All computations were performed with the G98 quantum-chemistry program package [43], and the DFT-B3LYP method [44–46] and LanL2DZ basis set [47] were adopted. The full geometry-optimization computations for the singlet ground states of these complexes were carried out. The stereographs of some related frontier molecular orbitals of the complexes **1** and **2** were drawn with the Molden v3.7 program [48] by means of the obtained computational results to illustrate the details of the frontier-molecular-orbital interactions (*Fig. 3*).

REFERENCES

[1] L. N. Ji, X. H. Zou, J. G. Liu, *Coord. Chem. Rev.* **2001**, *216–217*, 513.
[2] P. P. Pelligrini, J. R. Aldrich-Wright, *J. Chem. Soc., Dalton Trans.* **2003**, 176.
[3] C. Metcalfe, J. A. Thomas, *Chem. Soc. Rev.* **2003**, *32*, 215.
[4] J. A. Smith, J. G. Collins, B. T. Patterson, R. F. Keene, *J. Chem. Soc., Dalton Trans.* **2004**, 1277.
[5] P. U. Maheswari, M. Palaniandavar, *Inorg. Chim. Acta.* **2004**, *357*, 901.
[6] X. J. Yang, F. Drepper, B.Wu, W. H. Sun, W. Haehnel, C. Janiak, *J. Chem. Soc., Dalton Trans.* **2005**, 256.
[7] M. Narra, P. Elliott, S. Swavey, *Inorg. Chim. Acta* **2006**, *359*, 2256.
[8] D. Lawrence, V. G. Vaidyanathan, B. U. Nair, *J. Inorg. Biochem.* **2006**, *100*, 1244.
[9] D. B. Hall, R. E. Holmlin, J. K. Barton, *Nature (London, U.K.)* **1996**, *382*, 731.
[10] L. Mishra, A. K. Yadaw, S. Srivastava, A. B. Patel, *New J. Chem.* **2000**, *24*, 505.
[11] Y. J. Liu, H. Chao, Y. X. Yuan, H. J. Yu, L. N. Ji, *Inorg. Chim. Acta* **2006**, *359*, 3807.
[12] G. Yang, J. Z. Wu, L. Wang, L. N. Ji, X. Tian, *J. Inorg. Biochem.* **1997**, *66*, 141.
[13] Y. J. Liu, H. Chao, L. F. Tan, Y. X. Yuan, W. We, L. N. Ji, *J. Inorg. Biochem.* **2005**, *99*, 530.
[14] L. F. Tan, H. Chao, H. Li, Y. J. Liu, B. Sun, W. Wei, L. N. Ji, *J. Inorg. Biochem.* **2005**, *99*, 513.
[15] Y. Xiong, L. N. Ji, *Coord. Chem. Rev.* **1999**, *189*, 1.
[16] M. J. Frisch, A. Frisch, J. B. Foresman, Gaussian 94 User's Reference, Gaussian Inc., Pittsburgh, PA, 1994–1995.
[17] S. R. Stoyanov, J. M. Villegas, D. P. Rillema, *Inorg. Chem.* **2002**, *41*, 2941.
[18] N. Kurita, K. Kobayashi, *Compt. Chem.* **2000**, *24*, 351.
[19] E. A. Steck, A. R. Day, *J. Am. Chem. Soc.* **1943**, *65*, 452.
[20] R. B. Nair, E. S. Teng, S. L. Kirkland, C. J. Murphy, *Inorg. Chem.* **1998**, *37*, 139.
[21] S. Zails, V. Drchal, *Chem. Phys.* **1987**, *118*, 313.
[22] J. Z. Wu, B. H. Ye, L. Wang, L. N. Ji, J. Y. Zhou, R. H. Li, Z. Y. Zhou, *J. Chem. Soc., Dalton Trans.* **1997**, 1395.
[23] H. Xu, K. C. Zheng, L. J. Lin, H. Li, Y. Gao, L. N. Ji, *J. Inorg. Biochem.* **2004**, *98*, 87.
[24] R. E. Holmlin, J. A. Yao, J. K. Barton, *Inorg. Chem.* **1999**, *38*, 174.
[25] B. K. Ghosh, A. Chakra-Vorty, *Coord. Chem. Rev.* **1989**, *95*, 239.
[26] J. E. B. Johnson, R. R. Ruminski, *Inorg. Chim. Acta* **1993**, *208*, 231.
[27] J. K. Barton, A. Danishefsky, J. Goldberg, *J. Am. Chem. Soc.* **1984**, *106*, 2172.

[28] P. Lincoln, B. Norden, *J. Phys. Chem. B* **1998**, *102*, 9583.
[29] A. Wolf, G. H. Shimer Jr., T. Meehan, *Biochemistry* **1987**, *26*, 6392.
[30] a) A. M. Pyle, J. P. Rehmann, R. Meshoyrer, C. V. Kumar, N. J. Turro, J. K. Barton, *J. Am. Chem. Soc.* **1989**, *111*, 3051; b) Q. X. Zhen, B. H. Ye, Q. L. Zhang, J. G. Liu, H. Li, L. N. Ji, L. Wang, *J. Inorg. Biochem.* **1999**, *76*, 47.
[31] S. Satyanarayana, J. C. Dabroniak, J. B. Chaires, *Biochemistry* **1993**, *32*, 2573.
[32] Y. Xiong, X. F. He, X. H. Zou, J. Z. Wu, X. M. Chen, L. N. Ji, R. H. Li, J. Y. Zou, K. B. Yu, *J. Chem. Soc., Dalton Trans.* **1999**, *999*, 19.
[33] J. K. Barton, *Science (Washington, DC, U.S.)* **1986**, *233*, 727.
[34] K. Fukui, T. Yonezawa, H. Shingu, *J. Chem. Phys.* **1952**, *20*, 722; I. Fleming, 'Frontier Orbitals and Organic Chemical Reactions', Wiley, New York, 1976.
[35] K. C. Zheng, J. P. Wang, W. L. Peng, X. W. Liu, F. C. Yun, *J. Phys. Chem. A* **2001**, *105*, 10899.
[36] M. Yamada, Y. Tanaka, Y. Yoshimato, S. Kuroda, I. Shimao, *Bull. Chem. Soc. Jpn.* **1992**, *65*, 1006.
[37] J. N. Barddock, T. J. Meyer, *J. Am. Chem. Soc.* **1973**, *95*, 3158.
[38] B. P. Sullivan, D. J. Salmon, T. J. Meyer, *Inorg. Chem.* **1978**, *17*, 3334.
[39] M. F. Reichmann, S. A. Rice, C. A. Thomas, P. Doty, *J. Am. Chem. Soc.* **1954**, *76*, 3047.
[40] J. B. Chaires, N. Dattagupta, D. M. Crothers, *Biochemistry* **1982**, *21*, 3933.
[41] J. Marmur, *J. Mol. Biol.* **1961**, *3*, 208.
[42] G. Cohen, H. Eisenberg, *Biopolymers* **1969**, *8*, 45.
[43] M. J. Frisch, G. W. Trucks, H. B. Schlegel, G. E. Scuseria, M. A. Robb, J. R. Cheeseman, V. G. Zakrzewski, J. A. Montgomery Jr., R. E. Stratmann, J. C. Burant, S. Dapprich, J. M. Millam, A. D. Daniels, K. N. Kudin, M. C. Strain, O. Farkas, J. Tomasi, V. Barone, M. Cossi, R. Cammi, B. Mennucci, C. Pomelli, C. Adamo, S. Clifford, J. Ochterski, G. A. Petersson, P. Y. Ayala, Q. Cui, K. Morokuma, N. Rega, P. Salvador, J. J. Dannenberg, D. K. Malick, A. D. Raghavachairi, J. B. Foresman, J. Cioslowski, J. V. Ortiz, A. G. Baboul, B. B. Stefanov, G. Liu, A. Liashenko, P. Piskorz, I. Komaromi, R. Gomperts, R. L. Martin, D. J. Fox, T. Keith, M. A. Al-Laham, C. Y. Peng, A. Nanayakkara, M. Challacombe, P. M. W. Gill, B. Johnson, W. Chen, M. W. Wong, J. L. Andres, C. Gonzalez, M. Head-Gordon, E. S. Replogle, J. A. Pople, Gaussian 98, Revision A 11.4, Gaussian, Inc., Pittsburgh PA, 2002.
[44] A. D. Becke, *J. Chem. Phys.* **1993**, *98*, 1372.
[45] A. Gorling, *Phys. Rev. A* **1996**, *54*, 3912.
[46] J. B. Foresman, E. Frisch, 'Exploring Chemistry with Electronic Structure Methods', Gaussian Inc., Pittsburgh, PA, 2nd edn., 1996.
[47] P. J. Hay, W. R. Eadt, *J. Chem. Phys.* **1985**, *82*, 270; P. J. Hay, W. R. Eadt, *J. Chem. Phys.* **1985**, *82*, 299.
[48] G. Schaftenaar, J. H. Noordik, *J. Comput.-Aided Mol. Design* **2000**, *14*, 123.

Received April 27, 2007